LIMNOLOGY and OCEANOGRAPHY

ASLO

Limnol. Oceanogr. 9999, 2024, 1–14

doi: 10.1002/lno.12583

In situ aerobic methane oxidation rates in a stratified lake

Zachary W. Hudspeth,[1*] **Joshua L. Morningstar**,[1] **Howard P. Mendlovitz**,[1] **Jennifer A. Baily**,[2] **Karen G. Lloyd**,[2] **Christopher S. Martens**[1]

[1]University of North Carolina at Chapel Hill, Chapel Hill, North Carolina, USA
[2]University of Tennessee, Knoxville, Tennessee, USA

Abstract

Microbial aerobic methane oxidation is an important sink for aquatic methane worldwide. Despite its importance to global methane fluxes, few aerobic methane oxidation rates have been obtained in freshwater or marine environments without imposing changes to the microbial community through use of ex situ methods. A novel in situ incubation method for continuous time-series measurements was used in Jordan Lake, North Carolina, during 2020–2021, to determine reaction kinetics for aerobic methane oxidation rates across a wide range of naturally varying methane (55–1833 nM) and dissolved oxygen (DO; 28–366 μM) concentrations and temperatures (17–30°C). Methane oxidation began immediately at the start of each of 21 incubations and methane oxidation rates were 1st order with respect to methane. The data density allowed for accurate calculation of 1st-order rate constants, k, that ranged from 0.018 to 0.462 h^{-1} ($R^2 > 0.967$). Addition of ammonium (20–45 μM) to natural concentrations ranging from 0.057 to 2.4 μM did not change aerobic methane oxidation rate kinetics, suggesting that the natural population of aerobic methane oxidizers in this eutrophic lake was not nitrogen limited. Values of k inversely correlated most strongly with initial DO concentrations ($R^2 = 0.82$) rather than temperature. Values for k increased with Julian day throughout our sampling period, suggesting seasonal influences on methane oxidation via responses to geochemical changes or shifts in microbial community abundance and composition. These experiments demonstrate a high variability in the enzymatic capacity for 1st-order methane oxidation rates in this eutrophic lake that is tightly and inversely coupled to oxygen concentrations. Measurements of in situ aerobic methane oxidation rate constants allow for the direct quantification and modeling of the microbial community's capacity for methane oxidation over a wide range of natural methane concentrations.

Methane is a potent greenhouse gas with an estimated 37 times greater warming potential than carbon dioxide over a 100-yr period (Derwent 2020). Atmospheric methane concentrations have more than doubled over the past 250 yr (Hamdan and Wickland 2016). While emissions of anthropogenic origin have increased dramatically during the Anthropocene (Jorgenson 2006), an estimated 35–53% of current atmospheric methane comes from natural aquatic sources, mostly from microbial production in aquatic environments including wetlands, tributaries, lakes and oceans (Hamdan and Wickland 2016; Rosentreter et al. 2021). However, microbes are also important sinks for methane that can drastically attenuate net methane release to the atmosphere across these aquatic environments (e.g., Reeburgh 2007; Oswald et al. 2016; Leonte et al. 2018).

Dissolved methane, dissolved oxygen (DO), dissolved inorganic nitrogen (DIN), and total phosphorus (TP) concentrations and temperature can be important controls on aerobic methane oxidation rates in freshwater environments. High DO concentrations have been previously observed to produce an inhibitory effect on microaerophilic facultative methanotrophic activity (Rudd et al. 1976; Thottathil et al. 2019). However, elevated DIN levels have been hypothesized to allow for an increase in methane oxidation in highly oxygenated lakes (Rudd et al. 1976; Nijman et al. 2021) and coastal waters (Sansone and Martens 1978). Recently, low TP levels have been demonstrated to limit methane oxidation in boreal lakes (Denfeld et al. 2016; Sawakuchi et al. 2021) and TP has been

*Correspondence: zachwill@live.unc.edu

Additional Supporting Information may be found in the online version of this article.

Author Contribution Statement: Zachary Hudspeth, lead author, contributed to the field research plus led data analysis, construction and editing of the manuscript. Joshua Morningstar and Howard Mendlovitz led the field research plus contributed to data analysis. Jennifer Baily and Karen Lloyd participated in field experiments, interpretation of field data and contributed to the construction and editing of the manuscript. Christopher Martens led the overall project, participated in experimental designs, interpretation of data and results plus contributed to the construction and editing of the manuscript.

Special Issue: Autonomous Instrumentation and Big Data: New Windows, Knowledge, and Breakthroughs in the Aquatic Sciences. *Edited by: Yui Takeshita, Heidi Sosik, Dominique Lefevre, Werner Eckert, Kevin C. Rose and Deputy Editors Julia C. Mullarney, Steeve Comeau, and Elisa Schaum.*

positively correlated to methane oxidation in temperate lakes (Thottathil et al. 2022). It is well known that methane oxidation rates are correlated to methane concentration (Kankaala et al. 2006) and that temperature can be a significant factor controlling methane oxidation, particularly when methane concentrations are at saturation (Lofton et al. 2014).

Methane-oxidizing microbial communities are subject to changing environmental conditions in freshwater lakes, including temperature, dissolved methane and DO concentrations, and nutrient availability (Rudd et al. 1976; Lofton et al. 2014; Thottathil et al. 2019). These controlling conditions vary temporally in situ and are also the conditions most frequently altered during ex situ or quasi-in situ (disturbance prior to in situ) oxidation rate measurements. Removing water parcels from natural conditions can cause temperature changes, degassing via pressure changes or air exposure, and bottle effects during incubation. Many methods also alter methane concentrations through intentional additions. In situ techniques requiring no such alterations will enhance our understanding of the response of aerobic methane oxidation rates to changing conditions in natural environments.

Typical methane oxidation rates calculated from ex situ/quasi-in situ experiments in freshwater lakes range widely under varying environmental conditions. Rates assuming 0^{th}-order kinetics are almost exclusively reported despite the fact that methane oxidation kinetics are generally 1^{st} order with respect to methane concentration ($R = k[CH_4]$, where k is the 1^{st}-order rate constant) in natural waters (Leonte et al. 2017; Chan et al. 2019; Thottathil et al. 2019). Zeroth-order rates are representative of instantaneous rates, or the instantaneous consumption at a specific methane concentration. As aerobic methane oxidation is 1^{st} order with respect to methane concentration, experiments measuring 0^{th}-order consumption rates with ex situ methane concentrations, either via intentional methane additions or accidental loss during collection/incubation, will result in "apparent" or "potential" rates (Jannasch 1975). Such instantaneous rate measurements may not be relevant across the range of methane concentrations found in most lakes. Measuring 1^{st}-order rate constants instead allows for generalization to any in situ methane concentration if other controlling parameters are considered. However, few previous studies have been able to measure rate constants, usually due to limitations in methane concentration measurement frequency. Experiments are typically conducted with five or less time-series methane concentration measurements and are generally modeled using linear regression assuming a 0^{th}-order rate process (e.g., Dumestre et al. 1999; Kankaala et al. 2006; van Grinsven et al. 2020). More robust determinations of aerobic methane oxidation rates and overall methane dynamics in freshwater systems thus require a higher frequency of in situ measurements.

Our work in Jordan Lake, North Carolina, builds on previous studies through the development and application of an in situ method for underwater time-series methane oxidation rate measurements, which can be used in or modified for use in almost any aquatic system. We describe a novel water incubation bag coupled with a submersible sensor array, the "iBag system," that overcomes many of the limitations of ex situ rate measurements, including degassing of dissolved methane and DO, as well as temperature changes. We use advanced sensors to measure temporal changes in the in situ concentrations of methane, DO, and temperature in experiments ranging in duration from hours to days. The aerobic methane oxidation rate results we present here are based solely on underwater, in situ measurements obtained during 21 incubation experiments performed over a 19-month period (20 March 2020 to 29 October 2021) in stratified, eutrophic Jordan Lake, located near Chapel Hill, North Carolina. To obtain versatile aerobic methane oxidation rate results, we fit the temporal methane losses during each incubation experiment to an exponential equation in order to obtain 1^{st}-order rate constants, k (h^{-1}). The determination of k allows for direct comparisons of aerobic methane oxidation across sites featuring different temperature and/or DO regimes and is a more robust reflection of the activities of the aerobic methanotroph community.

Methods

Study site

All aerobic methane oxidation rate experiments were performed at Crosswinds Boating Center, Jordan Lake, NC (35°44′36.9″N, 79°00′28.8″W). Jordan Lake is a heavily eutrophied, human-made, stratified lake that serves as a drinking water reservoir for central North Carolina. The lake's surface waters regularly experience algal blooms, which can lead to hypoxic conditions in the water column (e.g., Wiltsie et al. 2018). Recent measurements of total dissolved nitrogen and phosphorus by the NC Division of Water Resources during 2020 (NC DWR 2021) provided values of 0.97 and 0.04 mg L^{-1}, respectively, from a nearby sampling station. All of our experiments deployed a 22-liter iBag system from a floating dock, suspended at 3.5 m water depth over muddy bottom sediments at 4 m total water depth. This experimental depth choice ensured that the iBag system would not disturb bottom sediment while sampling then incubating ambient lake water with elevated methane concentrations, plus avoided anoxic bottom waters that may be found in stratified deeper waters during warmer summer months. The dock provided a secure anchor point for multiple iBag systems plus constant power for sensors and computers without having to use battery packs. The test site was located behind a breakwater in a no-wake zone, providing protection from significant boat wake disturbances.

The nearby sample site to Chapel Hill, North Carolina allowed us to continue fieldwork throughout the COVID-19 pandemic, while adhering to all state, local, and university guidelines. Experiments were conducted between March and November of both 2020 and 2021, during months when

methane concentrations were elevated due to microbial production in underlying sediments at warmer seasonal temperatures. Data are absent from the end of July through October as water temperatures exceeded limits for our laser methane sensor, typically at an ambient water temperatures above approximately 30°C.

Experimental setup and execution

The iBag system (Fig. 1) used in this project allowed for continuous in situ measurements of methane and oxygen concentrations and temperature, plus collection of discrete water samples for microbial community analysis, plus the addition of and measurement of dissolved ammonium concentrations. We did not measure soluble reactive phosphorus. The 22-liter mylar incubation bag or iBag, impermeable to light and gas (Chan et al. 2016), was connected via low gas-permeable polyethylene tubing in series with a Laser Methane Sensor (Franatech GmbH), an oxygen optode (AADI 4330), circulation pump (SBE 5 M), and a water sampling port (Fig. 1). Both the laser methane sensor and the oxygen optode were encased in flow-through, pressure-sealed housings to create an air and water-tight closed system (Fig. 1).

The iBag system was operated in open-loop mode for drawing in, mixing, and equilibrating the iBag with ambient lake water, then switched to closed-loop mode for conducting incubation experiments. Trapped air bubbles in all components and tubing were removed as thoroughly as possible via physical manipulation to ensure that changes in dissolved gas concentrations resulted from microbial activity rather than through bubble stripping or air bubble dissolution. After removal of air bubbles, the system was left in open-loop mode for multiple hours at a pumping rate of 25 mL s^{-1}, to allow the iBag to completely mix with ambient water.

Aerobic methane oxidation rate experiments were conducted in closed-loop mode to initiate the incubation and to allow for continuous, time-series monitoring of methane and oxygen concentration and temperature. Discrete samples for dissolved ammonium and microbial community analyses were collected by syringe from a port on the iBag. Oxygen optode measurements at 1-min intervals were stored on an Aanderaa SeaGuard data logger. Dissolved methane concentrations were measured continuously and recorded internally on the underwater laser methane sensor at 1-min intervals. Instantaneous laser measurements were visualized in real-time through a software linkage to the sensor. Multiple iBag systems could be deployed simultaneously and incubation experiments lasted from several hours to several days. All systems were thoroughly flushed with freshwater and visually inspected for algal growth between separate experiments. After several days of experiments, each individual iBag system was broken down to component parts, each component physically scrubbed and thoroughly flushed again with freshwater before the next experiment. Mylar bags were replaced when flushing in open-loop mode with freshwater and/or physical scrubbing produced particles or color change.

Several blank experiments were conducted following ambient lake water experiments to confirm both the minimal presence of residual microbes between experiments and no systematic removal of methane. Two iBag systems were physically scrubbed, then flushed and filled with local tap water containing approximately 23 nM of methane to incubate for over 2 d to detect residual microbial activity or methane loss across tubing/housings. No decreases in methane occurred.

Dissolved ammonium was added via the sampling port to determine potential microbial N-limitation in oxygenated waters. After switching to closed-loop mode, 10 or 20 mL of ammonium standard (1000 μg mL^{-1}) was added to the iBag to elevate aqueous ammonium concentration to a target of 25 or 50 μM, respectively. Target DIN levels of > 20 and > 40 μM were chosen based on seasonal thresholds, described by Rudd et al. (1976), needed to overcome inhibition of aerobic methane oxidation at oxygen concentrations > 32 μM. After allowing the addition to mix, samples were collected and analyzed for ammonium concentration. A control with natural ammonium concentration was run simultaneous; incubations were run for approximately the same duration.

Sensors and laboratory analyses

DO measurements

DO concentrations were measured with Aanderaa Data Instruments (AADI) Series 4330 oxygen optodes using dynamic

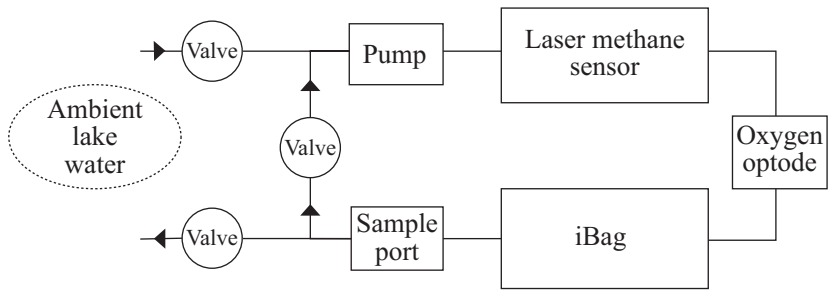

Fig. 1. iBag system created for in situ incubation experiments: 22-liter Mylar bag (iBag) in plastic housing which contains over 95% of the water within the system. The pump, laser methane sensor, and oxygen optode were housed in flow-through pressure-sealed caps. The sample port was used to subsample or make additions to the system. See Supporting Information Fig. S2 for photo of the system.

luminescence quenching. All optodes were calibrated annually before spring/summer deployments in our laboratory in batches of seven against micro-Winkler measurements in a water bath, achieving a precision of $\pm 2\,\mu$M, in agreement with values stated by AADI. Use of optodes allowed for continuous in situ measurements of DO and water temperature without the sensor oxygen consumption associated with Clark-type sensors (Bittig et al. 2018).

Methane measurements

Methane concentrations during iBag experiments were determined using the Franatech GmbH Laser Methane Sensor (LMS) with a specialized diode and gas permeable membrane inlet. Laboratory calibrations against capillary gas chromatography, using flame ionization, yielded a laser response linearly proportional to methane over a concentration range of 10 ppmv up to a cutoff factory value set to 10,000 ppmv. The LMS measured ppmv values were converted to nM concentration units using methane solubility data (Wiesenberg and Guinasso 1979). The detection limit for dissolved methane was less than 1 nM with a precision of $\pm$ 2 nM at concentrations greater than 5 nM at a constant flow rate of 25 mL s^{-1} (Supporting Information Fig. S1). Use of LMS sensors enabled continuous underwater concentration measurements while operating at low power consumption (< 12 W). Each LMS is designed for deep-sea work and housed in an approximately 41 cm length by 11 cm diameter titanium cylinder interfaced with the iBag system. The LMS has an internal temperature limit of 35°C, leading to overheating during summer months as mentioned above. The LMS is equilibrated to aqueous methane concentrations by pumping water across the LMS membrane at a constant flow rate of 25 mL s^{-1}.

Aqueous ammonium measurements

Ammonium was measured in discrete samples using the fluorometric technique described by Hu et al. (2014), which allowed for accurate analysis of relatively small volumes. Next, 60 mL samples were collected during closed-loop incubations and stored on ice or in a refrigerator in two 30-mL amber bottles.

Table 1. Experiment dates, duration, temperature, rate constant, R^2, and RMSE for all 26 incubation experiments. Experiments were conducted from 20 March 2020 through 29 October 2021. SF indicates that a sensor failure, either the oxygen optode (includes temperature) and/or LMS. Mean values are presented at the bottom.

Experiment	Date	Duration (h)	Mean temperature (°C)	Rate constant (h^{-1})	R^2	RMSE
1	20 Mar 2020	—	SF	SF	—	—
2	20 Mar 2020	45.80	SF	0.021	0.9948	0.44
3	24 Mar 2020	—	SF	SF	—	—
4	30 Mar 2020	45.58	16.69	0.019	0.9668	0.46
5	14 Apr 2020	15.84	18.35	0.051	0.9982	0.52
6	20 Apr 2020	51.87	SF	0.080	0.9943	3.22
7	26 Apr 2020	—	SF	SF	—	—
8	27 Apr 2020	44.68	18.97	0.035	0.9967	0.80
9	5 May 2020	50.65	SF	0.049	0.9975	0.41
10	12 May 2020	54.07	19.34	0.078	0.9984	1.01
11	16 Jun 2020	211.78	23.76	0.063	0.9893	28.47*
12	16 Jun 2020	107.08	23.53	0.075	0.9976	19.89*
13	26 Jun 2020	52.99	26.74	SF	—	—
14	26 Jun 2020	43.94	26.96	0.125	0.9906	4.36
15	29 Jun 2020	7.03	27.18	SF	—	—
16	29 Jun 2020	24.03	27.68	0.048	0.9988	6.18
17	17 Jul 2020	31.52	30.63	0.154	0.9961	2.35
18	26 Oct 2020	2.00	20.16	0.327	0.9976	2.38
19	26 Oct 2020	22.72	20.28	0.462	0.9993	1.50
20	26 Oct 2020	24.07	20.29	0.448	0.9974	3.42
21	25 Jun 2021	62.62	26.81	0.089	0.9984	2.31
22	29 Jun 2021	50.77	27.59	0.033	0.9995	1.10
23	10 Jul 2021	22.84	28.29	0.234	0.9872	1.07
24	29 Oct 2021	37.55	20.04	0.236	0.9997	1.07
25	29 Oct 2021	38.52	19.92	0.220	0.9988	2.14
26	29 Oct 2021	39.34	19.90	0.231	0.9993	1.61
Mean		47.27	23.16	0.147	0.9951	1.91

*High RMSE values likely due to outliers (> 3 SD from adjacent measurement) recorded by LMS, as seen in Fig. 2.

Within 12 h, 20 mL aliquots of samples or standards were filtered through 0.20-μm nylon membrane filters and reacted with 5 mL of *o*-phthalaldehyde reagent for 2.5–8 h. Samples and standards were then split into three replicates in 10-mL cylindrical cuvettes ($\sim$ 8 mL each) and measured for fluorescence averaged over a 10 s reading. Beers Law calculations were used to determine dissolved ammonium concentrations. The standard curve range utilized varied depending upon expected ammonium concentrations over three concentration ranges: low (25–200 nM), middle (200 nM to 2 μM), and high (2–400 μM). Samples with unknown concentrations were initially analyzed against the lowest calibration curve and then diluted if necessary. Standard deviations were calculated for all samples.

Rate constant calculations

Exponential fits were determined using nonlinear least squares regression using the Levenberg–Marquadt method of the form: $[CH_4] = Ae^{-kt} + \theta$ for experimental methane time-series data. A is methane concentration (nM), k is the modeled 1st-order rate constant (h^{-1}), and θ is the error term. The modeled initial methane concentration is $A + \theta$. The error term accounts for differences in LMS baseline settings. The precision of 1st-order rate constant, k, fits to the methane data from each experiment was determined by calculating the R^2 and root mean square error (RMSE) values for each experiment. Instantaneous rates were calculated from the rate constant multiplied by the initial methane concentration ($[CH_4]_{initial} * k$) to determine rate estimates in units of nM h^{-1}. Linear least squares regression was used to determine the rate of oxygen consumption and rate of ammonium production (Table 2).

Software

MATLAB Version: 9.14 (2023a) was used for all analyses and modeling (https://www.mathworks.com). In order to

Table 2. Initial methane, oxygen, and ammonium concentration and rate data for all experiments. SF indicates sensor failure of either the oxygen optode or the LMS for that experiment. Rate of oxygen consumption is calculated using linear regression.

Experiment	Modeled initial methane (nM)	Initial rate (nM h^{-1})*	Initial oxygen (μM)	Rate of oxygen loss (μM h^{-1})	Initial ammonium (nM)	Rate of ammonium production (nM h^{-1})
1	SF	—	SF	—	—	—
2	94.37	2.01	SF	—	—	—
3	SF	—	SF	—	—	—
4	94.46	1.77	365.82	1.62	—	—
5	100.64	5.10	229.50	4.59	—	—
6	290.03	21.81	SF	—	—	—
7	SF	—	SF	—	—	—
8	77.41	2.74	322.60	2.56	—	—
9	55.25	2.68	SF	—	—	—
10	111.45	8.71	310.24	3.67	—	—
11	1398.41	88.49	231.84	1.02	446.6	27.0
12	1833.30	138.10	185.76	1.71	425.7	20.5
13	SF	—	125.03	2.48	—	—
14	200.74	25.03	180.98	4.27	166.6	132.9
15	SF	—	27.64	3.93	—	—
16	914.52	44.11	141.71	6.32	2446.9	383.4
17	195.51	30.13	181.96	6.57	—	—
18	334.07	109.23	69.53	1.38	—	—
19	334.60	154.65	64.40	3.06	—	—
20	369.88	165.60	69.80	3.06	—	—
21	301.60	27.03	275.02	4.07	0.0**	246.4
22	364.13	12.10	280.21	5.79	57.4	370.3
23	79.35	19.08	115.05	3.62	544.5	157.2
24	327.93	77.52	145.69	0.86	—	—
25	333.83	73.43	164.36	0.98	—	—
26	347.38	80.12	155.51	0.91	—	—
Mean	388.52	51.88	182.13	3.12	681.3	191.1

*Initial rate is the rate constant multiplied by the initial methane concentration for comparison with typically used units.
**Concentration was below detection limits.

compare our *k* values, we calculated 1st-order rate constants using the same exponential model in this study from methane concentration time-series in a seasonally stratified Canadian lake from the data of Bogard et al. (2014) via WebPlotDigitizer (https://automeris.io/WebPlotDigitizer). Data and code used can be found at: https://github.com/zhudspeth/JordanLakePaper.

Results

Out of 26 total attempted experiments at the Jordan Lake site, 21 successfully measured temporal methane changes and 18 successfully measured temporal methane and oxygen concentrations in incubations of up to 212 h over a period of 19 months during 2020 to 2021 (Table 1; available data from incomplete experiments included). Across all incubations, temperature ranged from 16.7 to 30.36°C; initial methane concentrations ranged from 55 to 1833 nM; and DO ranged from 64 to 366 μM (Table 2). Methane concentration changes during incubations were fitted with exponential equations to yield 1st-order rate constants for each successful experiment.

Ammonium measurements were made throughout seven experiments (Table 2). Rates of oxygen consumption and ammonium production were calculated using linear models. Instantaneous rates of methane consumption were calculated for each experiment for comparison to previously published 0th-order rates.

Aerobic methane oxidation rate constants (*k*)

Aerobic microbial consumption of methane began immediately after switching to the closed-loop configuration regardless of seasonal ranges in temperature (17–31°C), initial methane and DO concentrations, or low (< 1 μM) ammonium concentrations.

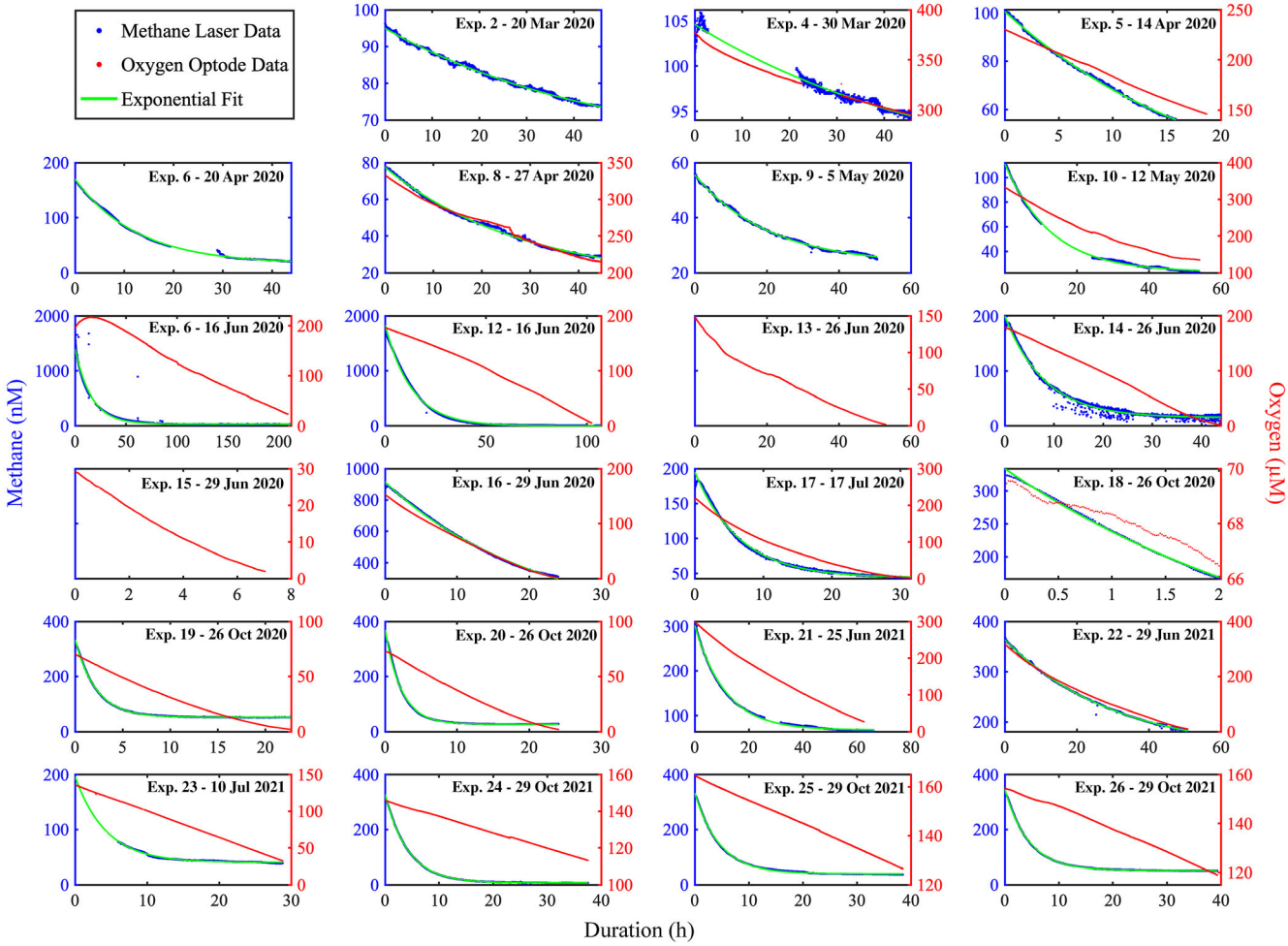

Fig. 2. Methane (dark blue) with exponential fits (green) and DO (red) concentration changes during iBag in situ aerobic methane oxidation incubations. Methane concentrations (left *y*-axis), oxygen concentrations (right *y*-axis), and duration (*x*-axis) varied across all experiments. Experiments 1, 3, and 7 are excluded due to sensor failure of both LMS and oxygen optodes. Experiments 2, 6, and 9 have no oxygen optode measurements due to sensor failure. Experiments 13 and 15 have no methane data due to sensor failure but exhibit respiration of oxygen. Individual plots in Supporting Information Figs. S3–S23.

Rate constants calculated from the measured losses in methane concentration for each experiment (Fig. 2), ranged from 0.019 to 0.462 h^{-1} (Table 1). The high temporal resolution of methane measurements obtained in the experiments allowed for a minimum R^2 value of 0.967 for modeled aerobic methane oxidation rates across all experiments. RMSE values show a good fit for the model for all experiments (Table 1). Three experiments had both LMS and oxygen optode sensor failure (experiments 1, 3, 7), two had only LMS sensor failures (Exp. 13, 15), and three had only oxygen optode sensor failure (experiments 2, 6, 9).

DO and ammonium during methane oxidation

DO consumption rates for each experiment were calculated from a linear fit of the oxygen data (Table 2). Consumption of DO began immediately when switched to closed-loop mode (Figs. 2, 3), and decreased linearly throughout the incubation. Incubations were typically concluded upon reaching anoxic conditions (< 2 μM).

Naturally occurring increases in dissolved ammonium that resulted from organic matter respiration were measured to seek potential impacts on aerobic methane oxidation due to nitrogen limitation (Fig. 3). Initial ammonium concentrations in experiments 11, 12, 14, 16, 19, 20, 22, and 23 rose linearly from initial values of 0.057 to 2.45 μM (Table 2). In experiment 21, initial ammonium was below the detection limit (listed as 0.0 in Table 2). During the incubations, the highest level of aqueous ammonium reached was 9.21 μM (end of experiment 16) and 9.85 μM (end of experiment 21).

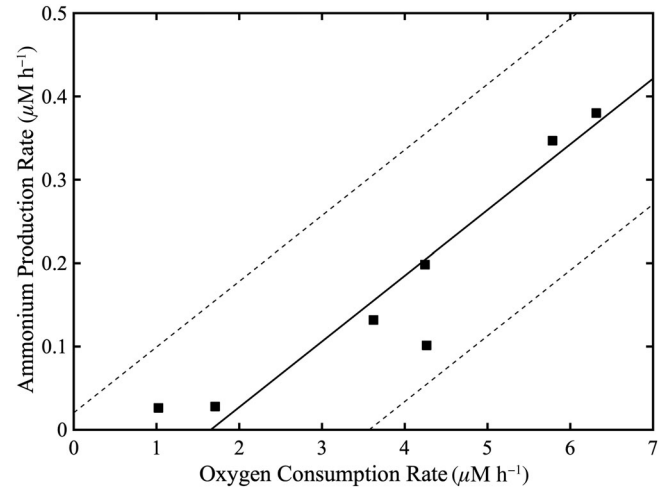

Fig. 4. Ammonium production rate vs oxygen consumption rate (squares) for seven experiments where both were measured. The linear model (solid line) has a slope of 12.7 and an R^2 of 0.87. The data fall mostly within the standard error (dashed line) of the model.

Rate of oxygen consumption correlates to the rate of ammonium produced (Fig. 4). The slope of the linear model is 12.7.

DIN additions

Ammonium addition experiments were conducted in conjunction with experiments 21, 22, and 23 to investigate the potential for DIN limitation on aerobic methane oxidation. In experiments 21 and 22, three iBag systems were deployed, one served as the control (Table 1; Figs. 2, 5a,b) and two were

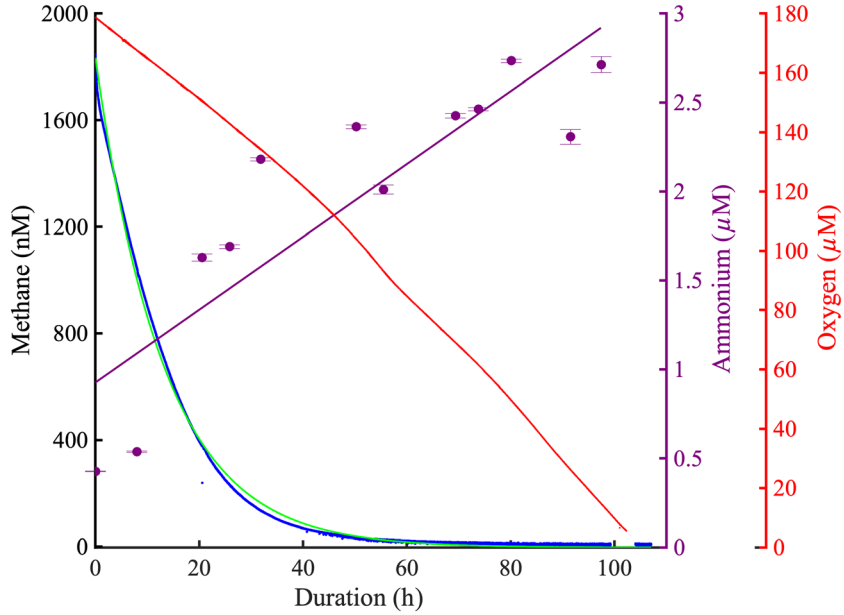

Fig. 3. Experiment 12 (from Fig. 2). Methane (blue) and oxygen (red) concentration measurements with methane oxidation rate model (green). Discrete ammonium samples (purple points) with error bars of three standard deviations at every point and a linear ammonium production rate fit (purple line).

injected with ammonium at the beginning of each experiment (Fig. 5a,b). These iBag incubations started with high initial oxygen concentrations ranging from 257 to 280 μM. In experiment 23, two iBags systems were deployed, one control (Table 1; Figs. 2, 5c) and one ammonium addition (Fig. 5c), starting with lower oxygen concentrations of 115 and 134 μM, respectively.

Dissolved ammonium concentration in the control for experiment 21 was below our detection limit at the start of the incubations. After ammonium additions and mixing, the two addition-iBags had ammonium concentrations of 20.5 and 21.9 μM. In Experiment 22, the control dissolved ammonium concentration was 57 nM, while the addition-iBags had measured ammonium concentrations of 43.4 and 45.2 μM after mixing. In experiment 23, the control dissolved ammonium concentration was 545 nM and the addition-iBag had an ammonium concentration of 38.4 μM after mixing.

Slight differences were observed between methane oxidation rates in the control incubation and ammonium addition incubations (Fig. 5). In experiment 21, methane oxidation rates in both addition experiments were lower than the control. In experiments 22 and 23, methane oxidation rates in ammonium addition experiments was slightly higher than in the control.

Effect of initial DO concentration on methane oxidation

A plot of our 1st-order rate constants for aerobic methane oxidation rate constants (Table 1) vs. the natural log of initial DO concentrations during 18 iBag experiments (Table 2) yields a significant negative correlation (Fig. 6). The strong inverse relationship between aerobic methane oxidation rate constants and DO concentrations between 64 and 365 μM

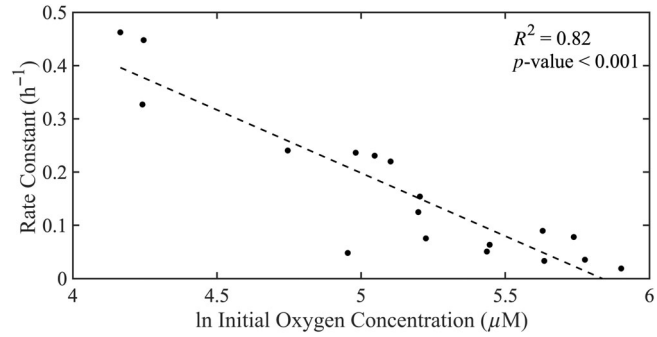

Fig. 6. Aerobic methane oxidation rate constants plotted against the natural log of initial oxygen concentrations for the 18 iBag experiments with methane and oxygen measurements. Bullet points represent individual experiments. The dashed line is a linear regression of the data.

supports the hypothesis that the methanotrophic population in low DO environments may be better poised to oxidize methane than the population that is active at higher DO concentrations. This agrees with previous experiments suggesting that methanotrophic bacteria are microaerophilic (Rudd et al. 1976; Guerrero-Cruz et al. 2021).

Temperature effect on methane oxidation

Consistent with Lofton et al. (2014), we were unable to distinguish a direct effect between temperature and rate constant values over the 18 experiments (Supporting Information Fig. S24). Communities of aerobic methanotrophs have an optimal temperature range between 10°C and 35°C (Islam et al. 2020). All experiments in this study were conducted within this broad range, potentially explaining our observed lack of temperature dependence. However, our study does

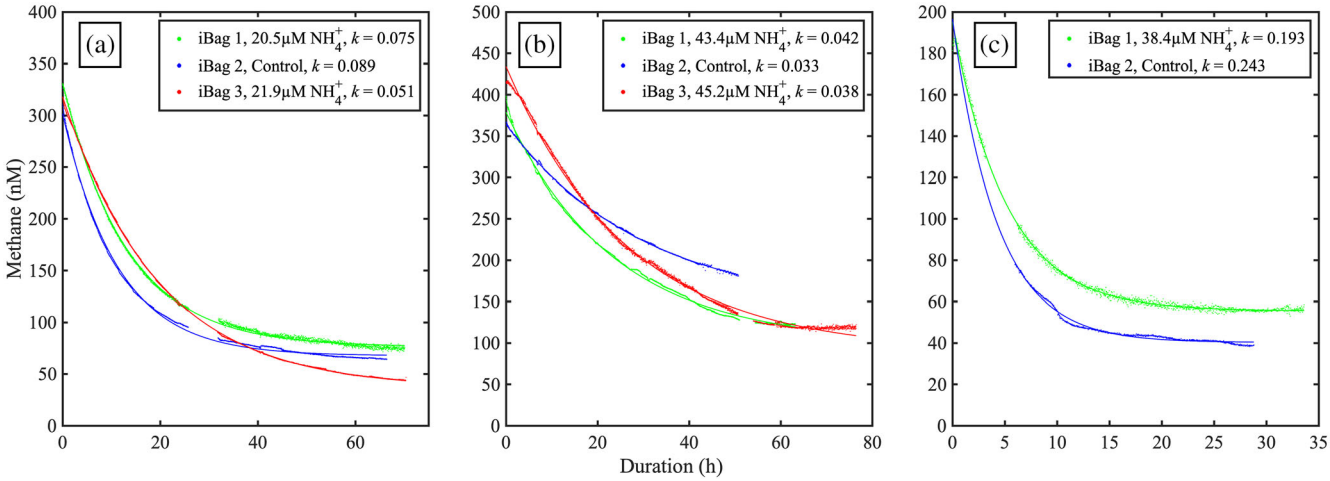

Fig. 5. Analysis of the effect of DIN on methane oxidation in three separate experiments with multiple iBag systems run per experiment. Ammonium was injected into two (**a**,**b**) or 1 (**c**) iBag(s) with another iBag serving as a control. Each color (red, green, blue) represents an individual iBag system: the green and red lines represent experiments injected with ammonium and the blue lines represent the controls. Control iBags are additionally found in Fig. 2 and Table 1. Rate constant, k, has units of (h^{-1}). Initial ammonium values for addition experiments are listed with experiment label. The scales of methane concentrations (y-axis) and duration (x-axis) are different for each individual plot.

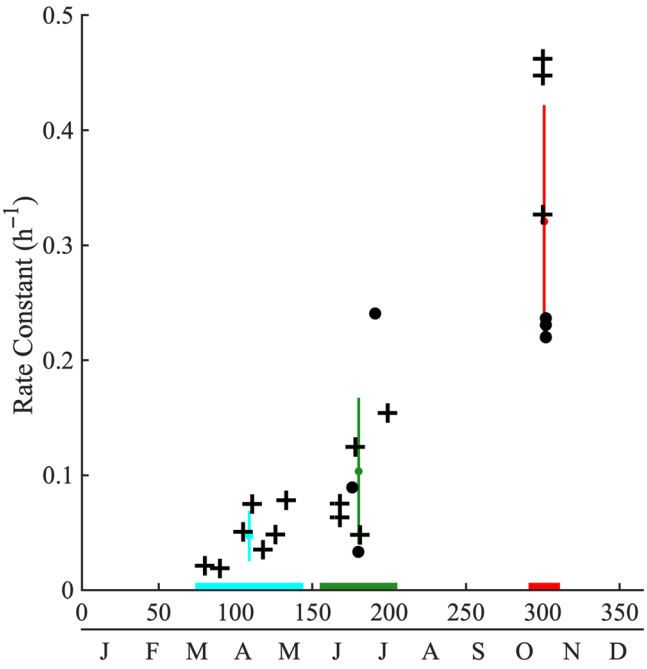

Fig. 7. Aerobic methane oxidation rate constants plotted against the Julian day of the experimental start. Colors represent groups of data points for spring (March–May: cyan), summer (June–July: green), and fall (October: red). Data were not collected during other months. The bottom color band approximately spans the Julian day of the data within each group. The vertical bars represent standard deviation of all points within the group. Data collected in 2020 are + symbols, data collected in 2021 are ● symbols.

indicate a potential relationship between aerobic methane oxidation rates and Julian day across the 19-month time span (Fig. 7). The spring, summer, and fall temperatures in Jordan Lake typically remain within the optimal range for aerobic methanotrophy, suggesting that seasonal variations in natural conditions not measured in this study affect aerobic methane oxidation.

Discussion

Our study sought to measure the kinetics of aerobic methane oxidation in a natural aquatic system through in situ time-series measurements that used advanced sensors to obtain high temporal resolution datasets. The calculated in situ rate constants allow us to gain new insights into methane dynamics within a stratified lake. The iBag system measurements included in situ methane and oxygen concentrations, ambient temporal temperature changes, and changes in DIN concentrations during incubations. The iBag system allows for discrete chemical and biological sampling throughout the duration of the experiment without deviation from in situ environmental conditions, thus allowing for the direct measurement of methane oxidation in almost any natural aquatic setting. The LMS and oxygen optode are housed in titanium cylinders and can be used for experiments at high pressures, for example, deep lakes and ocean seafloor deployments. To better accommodate temperate or tropical aquatic systems, the LMS housing could be modified to allow for more heat dissipation and full functionality in water temperatures consistently over 30°C. The high-frequency methane concentration measurements enabled our shortest experiment, 2 h duration, to be modeled with an R^2 of 0.9976. However, that experiment consumed almost 50% of the total methane within those 2 h. Based on the results of our experiments in Jordan Lake, North Carolina, we recommend an incubation time of at least 24 h or 50% methane consumption to ensure attainment of accurately modeled rate constants.

All 21 of our experiments with an operating LMS demonstrate aerobic methane oxidation as having 1st-order kinetics. The 1st-order relationship of methane concentration to aerobic methane oxidation was expected as previously observed (Leonte et al. 2017; Chan et al. 2019; Thottathil et al. 2019), although our work confirmed these results with a denser and more easily modeled dataset. The 1st-order kinetics found for methane consumption in Jordan Lake implies that the process is enzymatically catalyzed. In all 18 experiments with both methane and oxygen concentration time-series data, the decrease in methane was accompanied by a decrease in DO, as no photosynthesis should occur due to the absence of light in the iBags. In experiment 11, tiny air bubbles not removed during experimental set-up likely contributed to an initial increase in oxygen before decreasing at a rate consistent with other experiments (Fig. 2).

Methane oxidation and DO consumption

DO consumption rates were orders of magnitude higher than initial instantaneous aerobic methane oxidation rates (Table 2), presumably fueled largely by total microbial community respiration of dissolved organic matter (DOM) and particulate organic matter (POM) in the turbid lake waters. Aerobic methane oxidation consumes 1 mol of CH_4 per 2 mol of O_2 thus having a stoichiometry of 1:2. Therefore, in Jordan Lake, aerobic methane oxidation is not responsible for a significant decrease in oxygen concentrations and accounts for less than 2% of total DO consumption. Furthermore, this hypothesis is supported by a 12.7 ratio of DO consumption to DIN production, which is reflective of typical C : N ratios found in lakes. A ratio between 10 and 20 is expected if the majority of DO consumption is fueled by a mixed terrestrial/planktonic organic matter source or by organic matter that has already undergone substantial decomposition (Kemp et al. 1977; Yustiawati et al. 2022). The ratio is slightly higher than some freshwater systems likely due to the high concentrations of POM and DOM present in Jordan Lake (NC DWR 2021).

Potential N limitation

Based on previous findings by Rudd et al. (1976), Sansone and Martens (1978), and Nijman et al. (2021); we expected elevated DIN levels to increase rates of methane oxidation,

especially under high oxygen concentrations (> 32 μM) where N_2 fixation might be inhibited. For experiments 21–23, the initial oxygen concentrations were above the threshold for the inhibitory effects seen by Rudd et al. (1976).

No large effect of DIN additions on aerobic methane oxidation during these experiments suggests that the microbial communities in Jordan Lake are not N-limited (Fig. 5). High total nitrogen levels measured in Jordan Lake support this hypothesis (NC DWR 2021). Both Rudd et al. (1976) and Sansone and Martens (1978) measured rates at higher initial methane concentrations, potentially impacting the overall DIN effect. In natural systems, methane concentration may be the limiting factor for aerobic methanotrophs as opposed to DIN. Rudd et al. (1976) performed incubations bubbled with a methane–air mixture to achieve methane concentrations exceeding 800 μM and oxygen concentrations below 31 μM to avoid oxygen inhibition. All three of our DIN addition experiments were above 31 μM DO but were within the range of the oxygen inhibition effect we measured.

Recent studies have demonstrated phosphorus availability limiting methane oxidation in freshwater lakes, where low TP levels inhibited methane oxidation across wide ranging methane and oxygen concentrations (Sawakuchi et al. 2021). We did not measure TP in this study. However, the iBag system is perfectly suited for future work on phosphorus limitations in a similar application to DIN in this study. The sampling port allows for discrete samples of water to be analyzed for TP or additions of TP to investigate the effects of methane oxidation.

Oxygen inhibition of aerobic methane oxidation

While aerobic methanotrophs require a minimum oxygen threshold to consume methane, the communities have previously been categorized as microaerophilic (Rudd et al. 1976; Thottathil et al. 2019; Guerrero-Cruz et al. 2021). We measured an inverse relationship between DO concentrations and rate constants over the entire range of DO: 64–365 μM (Fig. 6). This characteristic may either be an aversion to high oxygen concentrations or an adaptation to high methane environments, which tend to be anoxic as microbial methane production largely occurs anaerobically (Martens and Berner 1974; Reeburgh 2007). As methane oxidation here is aerobic, there is an optimal oxygen concentration for methane oxidation. Over the course of our study, initial ambient oxygen concentrations were not low enough to test the optimal oxygen concentration threshold; Thottathil et al. (2019) estimated the optimal oxygen concentration to be 14.9 μM. Our in situ measurements yielded a stronger inverse correlation ($R^2 = 0.82$) between the natural log of oxygen concentrations and rate constants than previous studies comparisons of oxygen concentrations and 0^{th}-order rates (Thottathil et al. 2019). As rate constants provide a more direct measurement of the methanotrophic communities' capacity for methane consumption than instantaneous rates, our findings support the hypothesis that there is an aversion to high oxygen among the methanotrophic communities. Therefore, lower oxygen concentrations likely support larger or more efficient populations of aerobic methanotrophs and thus provide a greater capacity for methane consumption.

Temporal variability of rate constants

Over the 19-month experimental period, our measured rate constants appeared to increase during the Julian year (Fig. 7). The measurement of rate constants allows us to decouple high methane concentrations from the capacity for methanotrophic consumption. While our highest methane concentrations are in the summer months of June and July, our rate constants were highest during late October/early November. We hypothesize that a buildup of methanotrophs throughout the year in Jordan Lake has a larger effect on aerobic methane oxidation rates than in situ temperature. We predict a positive correlation between the in situ rate constant and methanotrophic community size as previously seen in ex situ measurements by Reis et al. (2020). The methane consuming microbial community present in Jordan Lake may change seasonally in composition or size leading to a varying consumption capacity throughout the Julian year.

Previous seasonal studies of high latitude lakes have revealed similar increases in aerobic methane oxidation during months above the temperature threshold for methanotrophs (Martinez-Cruz et al. 2015). While geographic location and lake dynamics (such as annual ice coverage) make comparing seasonality to Jordan Lake difficult, both long term methane oxidation studies have demonstrated seasonal changes in aerobic methane oxidation. Multiple year coverage, microbial community measurements, and frequent rate constant measurements are required to fully understand seasonal methane oxidation dynamics in Jordan Lake and other aquatic ecosystems.

Comparison with previous aerobic methane oxidation rate studies

To our knowledge, all previous studies in freshwater lakes, apart from Thottathil et al. (2019), calculate and report aerobic methane oxidation in units of nM h^{-1}, μM d^{-1}, and so forth, as opposed to producing 1^{st}-order rate constants (h^{-1}). Thottathil et al. (2019) calculated k values that ranged from 0.002 to 0.063 h^{-1}. Although rate constants were not calculated by Bogard et al. (2014), we used their data to calculate k values that ranged from 0.003 to 0.021 h^{-1}. The lower limits of our measured rate constants fall within the previously measured range from Thottathil et al. (2019) and the calculated range from Bogard et al. (2014) data, respectively, although our largest rate constants are an order of magnitude higher. Both of these previous studies investigated lakes at higher latitudes. While the initial methane and oxygen concentrations

Table 3. Rates, temperature, experimental type, and initial methane concentration from previous measurements of aerobic methane oxidation in freshwater systems. The data were compiled using references from D'Ambrosio and Harrison (2021). Aerobic methane oxidation rate ranges were converted from original units to nM h^{-1} and represent the largest ranges reported.

Source*	Lake locations	Aerobic methane oxidation (nM h^{-1})	Temp (°C)	In situ/ ex situ/quasi	Initial CH_4 (nM)
This study	Jordan Lake, North Carolina	1.8–166	16–31	In situ	55–1833
Bastviken et al. (2008)	Wisconsin	7.1–262	5–25 C	Quasi-in situ	100–800,000
Bogard et al. (2014)	Montreal, California	3–8	20	Ex situ	100–530
Donis et al. (2017)	Lake Hallwil, Switzerland	0.13–0.15	20–25	Quasi-in situ	200–800
Duchemin et al. (2006)	Quebec, Canada	0.16–12	NA	Quasi-in situ	NA
Jannasch (1975)	Lake Kivu, Central Africa	20	22–25	Ex situ	18,750–50,000
Kankaala et al. (2006)	Valkea-Kotinen, Finland	1.7–75	10–18	Ex situ	0–2500
Kankaala et al. (2007)	Mekkojarvi, Finland	1.25–600	5–11	Ex situ	120–167,000
Lofton et al. (2014)	Alaska	2.2–340	0–16	Ex situ	33,000
Pasche et al. (2011)	Lake Kivu, Central Africa	25.75–45.7	NA	Ex situ	0–500,000
Reis et al. (2020)	Quebec, Canada	0.17–2740	5–25	Ex situ	10–455,000
Thottathil et al. (2019)	Quebec, Canada	0.42–1500	5–25	Ex situ	60–455,000

in all previous lake studies spanned a large range and incubation temperatures varied, each lake was sampled during a single day. Aerobic methane oxidation may be controlled by geochemical as well as microbial variables; the temporal variation we observed in our study suggests that rates observed at a single time point may not be indicative of a lake's fluctuating potential for aerobic methane oxidation.

A comparison of our instantaneous rate measurements (Table 2) with 0^{th}-order rates from previous studies using various methods in lake systems is presented in Table 3. Our instantaneous rates are within the ranges of previously reported (nM h^{-1}) rates.

Previous studies generally assumed 0^{th}-order kinetics, and modeled methane consumption as a linear decrease. A linear consumption of methane will underestimate the rate of methane consumption on shorter timescales and overestimate on longer timescales, leading to inaccurate estimates of overall temporal methane consumption in natural aquatic environments. When aerobic methane oxidation is measured using ex situ methane concentrations and assumed to be a 0^{th}-order process the rate will be highly dependent on the methane concentration and will not reflect the capacity for microbial consumption present in the water column. Measuring rate constants is more reflective of the 1^{st}-order response during incubation by the microbial methane-oxidizing community. Furthermore, dissolved methane concentrations in the water column are generally dependent on changes in sedimentary production and release via bubble ebullition or diffusion which are directly affected by temperature (e.g., Martens and Klump 1980; Schulz et al. 1997). Previous measurements of 0^{th}-order rates may show a temperature or other geochemical dependence because of variability in supply rate of dissolved methane and not microbial consumption. To understand temporal variation in aerobic methane oxidation in a freshwater aquatic system, datasets with enough resolution to calculate 1^{st}-order rate constants should be collected. Further in situ measurements of rate constants in key aquatic environments will enable more robust estimates of microbial consumption in global methane fluxes.

Conclusions

Microbial aerobic methane oxidation is an important sink for natural methane emissions worldwide. Despite its importance to global methane fluxes, experimental limitations may compromise ex situ methods for determining the importance of aerobic methane oxidation rates in local and global budgets. In particular, ex situ measurements may impose critical changes to the microbial community caused by removal from the natural environment during experimentation. Our incubation bag (iBag) method allows for simultaneous in situ aerobic methane oxidation, respiration and other biogeochemical rate measurements in aquatic environments ranging from ponds and lakes to coastal and deep ocean environments. Successful recent experiments at deep-sea sites (C.S. Martens unpubl.) have also provided data utilizing free vehicle benthic landers to deploy multiple iBag systems. Results from 21 in situ incubation experiments conducted in Jordan Lake has revealed that aerobic methane oxidation begins immediately and follows 1^{st}-order kinetics with respect to methane concentrations. First-order rate constants, k, determined for each experiment range from 0.018 to 0.462 h^{-1} with all model fits exceeding an R^2 value of 0.967. No correlation was found between rate constants and ambient temperature, however, rate constants varied seasonally, suggesting the microbial community may be more impactful than other

environmental conditions in determining the capacity of aerobic methane oxidation.

Less than 2 % of total DO consumption observed during our experiments was explained by methane oxidation. DO concentrations decreased at an average rate ~ 13 times that of ammonium production during incubations, suggesting respiration of N-depleted organic matter relative to the Redfield ratio, likely because of the higher input of terrestrial organic matter which tends to be N-depleted relative to fresh planktonic marine organic matter. Additions of ammonium had no effect on methane oxidation under multiple DO concentrations, suggesting that N is not limiting for methanotrophs in Jordan Lake.

Our methane oxidation rate constants, *k*, when multiplied by ambient methane concentrations (initial iBag concentrations), produce aerobic methane oxidation rate values within the range previously measured in freshwater lakes. Aerobic methane oxidation rate constants were inversely correlated with initial DO concentrations, suggesting that high DO concentrations may limit the efficacy of the biological filter on natural methane emissions in freshwater lakes. Aerobic methane oxidation rate constants can be used for temporal and spatial modeling across a wide range of natural methane concentrations and provide a powerful approach for understanding and quantifying microbial methanotrophy and other controls on aerobic methane oxidation under in situ conditions.

Data availability statement

The data that support the findings of this study are openly available in GitHub at https://github.com/zhudspeth/JordanLakePaper, reference number 465a96d.

References

Bastviken, D., J. J. Cole, M. L. Pace, and M. C. Van de-Bogert. 2008. Fates of methane from different lake habitats: Connecting whole-lake budgets and CH_4 emissions. Eur. J. Vasc. Endovasc. Surg. **113**: G02024. doi:10.1029/2007JG000608

Bittig, H. C., N. Körtzinger, C. Neill, E. van Ooijen, J. N. Plant, J. Hahn, K. S. Johnson, B. Yang, and S. R. Emerson. 2018. Oxygen optode sensors: Principle, characterization, calibration, and application in the ocean. Front. Mar. Sci. **4**: 429. doi:10.3389/fmars.2017.00429

Bogard, M., P. del Giorgio, L. Boutet, M. C. G. Chaves, Y. T. Prairies, A. Merante, and A. M. Derry. 2014. Oxic water column methanogenesis as a major component of aquatic CH_4 fluxes. Nat. Commun. **5**: 5350. doi:10.1038/ncomms6350

Chan, E. W., J. D. Kessler, A. M. Shiller, D. J. Joung, and F. Colombo. 2016. Aqueous mesocosm, techniques enabling real-time measurement of the chemical and isotopic kinetics of dissolved methane and carbon dioxide. Environ. Sci. Technol. **50**: 3039–3046. doi:10.1021/acs.est.5b04304

Chan, E. W., A. M. Shiller, D. J. Joung, E. C. Arrington, D. L. Valentine, M. C. Redmond, J. A. Breier, S. A. Socolofsky, and J. D. Kessler. 2019. Investigations of aerobic methane oxidation in two marine seep environments: Part 1—Chemical kinetics. J. Geophys. Res. Oceans **124**: 8852–8868. doi:10.1029/2019JC015594

D'Ambrosio, S., and J. Harrison. 2021. Methane production and oxidation rates in lakes and reservoirs. figshare [Dataset]. doi:10.6084/m9.figshare.12811778.v2

Denfeld, B. A., M. C. Canelhas, G. A. Weyhenmeyer, S. Bertilsson, A. Eiler, and D. Bastviken. 2016. Constraints on methane oxidation in ice-covered boreal lakes. Eur. J. Vasc. Endovasc. Surg. **121**: 1924–1933. doi:10.1002/2016JG003382

Derwent, R. G. 2020. Global warming potential (GWP) for methane: Monte Carlo analysis of the uncertainties in global tropospheric model predictions. Atmos. **11**: 486. doi:10.3390/atmos11050486

Donis, D., S. Flury, A. Stöckli, J. E. Spangenberg, D. Vachon, and D. F. McGinnis. 2017. Full-scale evaluation of methane production under oxic conditions in a mesotrophic lake. Nat. Commun. **8**: 1661. doi:10.1038/s41467-017-01648-4

Duchemin, É., M. Lucotte, R. Canuel, and N. Soumis. 2006. First assessment of methane and carbon dioxide emissions from shallow and deep zones of boreal reservoirs upon ice break-up. Lakes Reserv. Res. Manag. **11**: 9–19. doi:10.1111/j.1440-1770.2006.00285.x

Dumestre, J. F., J. Guézennec, C. Galy-Lacaux, R. Delmas, S. Richard, and L. Labroue. 1999. Influence of light intensity on methanotrophic bacterial activity in Petit Saut Reservoir, French Guiana. Appl. Environ. Microbiol. **65**: 534–539. doi:10.1128/AEM.65.2.534-539.1999

Guerrero-Cruz, S., A. Vaksmaa, M. A. Horn, H. Niemann, M. Pijuan, and A. Ho. 2021. Methanotrophs: Discoveries, environmental relevance, and a perspective on current and future applications. Front. Microbiol. **12**: 678057. doi:10.3389/fmicb.2021.678057

Hamdan, L. J., and K. P. Wickland. 2016. Methane emissions from oceans, coasts, and freshwater habitats: New perspectives and feedbacks on climate. Limnol. Oceanogr. **61**: S3–S12. doi:10.1002/lno.10449

Hu, H., Y. Liang, S. Li, Q. Guo, and C. Wu. 2014. A Modifiedo-Phthalaldehyde Fluorometric analytical method for ultra-trace ammonium in natural waters using EDTA-Naoh as buffer. J. Anal. Methods Chem. **2014**: 1–7. doi:10.1155/2014/728068

Islam, T., A. Gessesse, A. Garcia-Moyano, J. C. Murrell, and L. Øvreås. 2020. A novel moderately thermophilic type Ib methanotroph isolated from an alkaline thermal spring in the Ethiopian Rift Valley. Microorganisms **8**: 250. doi:10.3390/microorganisms8020250

Jannasch, H. W. 1975. Methane oxidation in Lake Kivu (central Africa). Limnol. Oceanogr. **20**: 860–864. doi:10.4319/lo.1975.20.5.0860

Jorgenson, A. K. 2006. Global warming and the neglected greenhouse gas: A cross-national study of the social causes of methane emissions intensity, 1995. Soc. Forces **84**: 1779–1798. doi:10.1353/sof.2006.0050

Kankaala, P., J. Huotari, E. Peltomaa, T. Saloranta, and A. Ojala. 2006. Methanotrophic activity in relation to methane efflux and total heterotrophic bacterial production in a stratified, humic, boreal lake. Limnol. Oceanogr. **51**: 1195–1204.

Kankaala, P., S. Taipale, H. Nykänen, and R. I. Jones. 2007. Oxidation, efflux, and isotopic fractionation of methane during autumnal turnover in a polyhumic, boreal lake. Eur. J. Vasc. Endovasc. Surg. **112**: G02033. doi:10.1029/2006JG000336

Kemp, A. L. W., R. L. Thomas, H. K. T. Wong, and L. M. Johnston. 1977. Nitrogen and C/N ratios in the sediments of Lakes Superior, Huron, St. Clair, Erie, and Ontario. Can. J. Earth Sci. **14**: 2402–2413. doi:10.1139/e77-205

Leonte, M., J. D. Kessler, M. Y. Kellermann, E. C. Arrington, D. L. Valentine, and S. P. Sylva. 2017. Rapid rates of aerobic methane oxidation at the feather edge of gas hydrate stability in the waters of Hudson Canyon, US Atlantic Margin. Geochim. Cosmochim. Acta **204**: 375–387. doi:10.1016/j.gca.2017.01.009

Leonte, M., B. Wang, S. A. Socolofsky, S. Mau, J. A. Breier, and J. D. Kessler. 2018. Using carbon isotope fractionation to constrain the extent of methane dissolution into the water column surrounding a natural hydrocarbon gas seep in the northern Gulf of Mexico. Geochem. Geophys. Geosyst. **19**: 4459–4475. doi:10.1029/2018GC007705

Lofton, D. D., S. C. Whalen, and A. Hershey. 2014. Effect of temperature on methane dynamics and evaluation of methane oxidation kinetics in shallow Arctic Alaskan lakes. Hydrobiologia **721**: 209–222. doi:10.1007/s10750-013-1663-x

Martens, C. S., and R. A. Berner. 1974. Methane production in the interstitial waters of sulfate-depleted marine sediments. Science **185**: 1167–1169. doi:10.1126/science.185.4157.1167

Martens, C. S., and J. V. Klump. 1980. Biogeochemical cycling in an organic-rich coastal marine basin—I. Methane sediment-water exchange processes. Geochim. Cosmochim. Acta **44**: 471–490. doi:10.1016/0016-7037(80)90045-9

Martinez-Cruz, K., A. Sepulveda-Jauregui, K. W. Anthone, and F. Thalasso. 2015. Geographic and seasonal variation of dissolved methane and aerobic methane oxidation in Alaskan lakes. Biogeosciences **12**: 4595–4606. doi:10.5194/bg-12-4595-2015

NC Division of Water Resources. 2021. Study for the ongoing assessment of water quality in B. Everett Jordan Lake, including identification of select emerging compounds: 2020 Results. Water Sciences Section, Intensive Survey Branch. Available from https://deq.nc.gov/media/26180/download?attachment

Nijman, T. P. A., and others. 2021. Warming and eutrophication interactively drive changes in the methane-oxidizing community of shallow lakes. ISME Commun. **1**: 32. doi:10.1038/s43705-021-00026-y

Oswald, K., J. Milucka, A. Brand, P. Hach, S. Littmann, B. Wehrli, M. M. M. Kuypers, and C. J. Schubert. 2016. Aerobic gammaproteobacterial methanotrophs mitigate methane emissions from oxic and anoxic lake waters. Limnol. Oceanogr. **61**: S101–S118. doi:10.1002/lno.10312

Pasche, N., and others. 2011. Methane sources and sinks in Lake Kivu. Eur. J. Vasc. Endovasc. Surg. **116**: G03006. doi:10.1029/2011JG001690

Reeburgh, W. S. 2007. Oceanic methane biogeochemistry. Chem. Rev. **107**: 486–513. doi:10.1021/cr050362v

Reis, P. C. J., S. D. Thottathil, C. Ruiz-González, and Y. T. Prairie. 2020. Niche separation within aerobic methanotrophic bacteria across lakes and its link to methane oxidation rates. Environ. Microbiol. **22**: 738–751. doi:10.1111/1462-2920.14877

Rosentreter, J. A., and others. 2021. Half of global methane emissions come from highly variable aquatic ecosystem sources. Nat. Geosci. **14**: 225–230. doi:10.1038/s41561-021-00715-2

Rudd, J. W., A. Furutani, R. J. Flett, and R. D. Hamilton. 1976. Factors controlling methane oxidation in shield lakes: The role of nitrogen fixation and oxygen concentration. Limnol. Oceanogr. **21**: 357–364. doi:10.4319/lo.1976.21.3.0357

Sansone, F. J., and C. S. Martens. 1978. Methane oxidation in Cape Lookout bight, North Carolina. Limnol. Oceanogr. **23**: 349–355. doi:10.4319/lo.1978.23.2.0349

Sawakuchi, H. O., G. Martin, S. Peura, S. Bertilsson, J. Karlsson, and D. Bastviken. 2021. Phosphorus regulation of methane oxidation in water from ice-covered lakes. Eur. J. Vasc. Endovasc. Surg. **126**: 8. doi:10.1029/2020JG006190

Schulz, S., H. Matsuyama, and R. Conrad. 1997. Temperature dependence of methane production from different precursors in a profundal sediment (Lake Constance). FEMS Microbiol. Ecol. **22**: 207–213. doi:10.1111/j.1574-6941.1997.tb00372.x

Thottathil, S. D., P. C. Reis, and Y. T. Prairie. 2019. Methane oxidation kinetics in northern freshwater lakes. Biogeochemistry **143**: 105–116. doi:10.1007/s10533-019-00552-x

Thottathil, S. D., P. C. Reis, and Y. T. Prairie. 2022. Variability and controls of stable carbon isotopic fractionation during aerobic methane oxidation in temperate lakes. Front. Environ. Sci. **10**: 833688. doi:10.3389/fenvs.2022.833688

van Grinsven, S., J. S. Damsté, A. A. Asbun, J. C. Engelmann, J. Harrison, and L. Villanueva. 2020. Methane oxidation in anoxic lake water stimulated by nitrate and sulfate

addition. Environ. Microbiol. **22**: 766–782. doi:10.1111/1462-2920.14886

Wiesenberg, D. A., and N. L. Guinasso. 1979. Equilibrium solubilities of methane, carbon monoxide, and hydrogen in water and sea water. J. Chem. Eng. Data **24**: 356–360. doi:10.1021/JE60083A006

Wiltsie, D., A. Schnetzer, J. Green, M. Vander Borgh, and E. Fensin. 2018. Algal blooms and cyanotoxins in Jordan Lake, North Carolina. Toxins **10**: 92. doi:10.3390/toxins10020092

Yustiawati, M. S. Syawal, and Rosidah. 2022. Carbon, nitrogen and C/N ration of sediment in a floodplain lake: Lake Tempre, South Sulawesi. IOP Conf. Ser. Earth Environ. Sci. **1062**: 012018. doi:10.1088/1755-1315/1062/1/012018

Acknowledgments

This work was primarily supported by the National Science Foundation Chemical Oceanography (OCE-1948720 to C.S.M and K.G.L.). Other funding came from the US DOE Office of Science (DE-SC0020369 to K.G. L.) and the National Academies Keck Futures Initiative (NAKFI A17-1286-001 to C.S.M). Statistical analysis of model fits to the methane time-series data presented here was performed after consultations with faculty and graduate student members of a statistics class at UNC-Chapel Hill. Experiments comply with existing laws of North Carolina and the United States.

Conflict of Interest

None declared.

Submitted 13 November 2023
Revised 20 March 2024
Accepted 14 April 2024

Associate editor: *Werner Eckert*